STATISTICS, OPTIMIZATION AND INFORMATION COMPUTING
Stat., Optim. Inf. Comput., Vol. **13**, January 2025, pp 158–172.
Published online in International Academic Press (www.IAPress.org)

Real-Time Scheduling Optimization of Integrated Energy Systems in Smart Grids based on Approximate Dynamic Programming

Dongzhao Wang [1,a], Yue Sun [1,a], Yan Wu [1,a], Zixuan Wang [1], Keliang Duan [2], Xiaoyun Tian [1,*], Dachuan Xu [1]

[1] *Institute of Operations Research and Information Engineering, Beijing University of Technology, China*
[2] *Beijing JH Eco-Energy Technology Co., LTD, China*

Abstract With the large-scale integration of renewable energy (RE) sources and rapid advancements in smart grid (SG) technologies, the efficient integration of diverse energy resources to achieve supply-demand balance and maximize cost-effectiveness has emerged as a research hotspot in the energy sector. This paper addresses the real-time scheduling challenge in integrated energy systems (IES) within the context of SG, emphasizing pivotal factors such as electric and thermal load scheduling, energy storage control, dynamic electricity pricing, carbon emission mechanisms, and demand response (DR). To this end, we propose a comprehensive scheduling model tailored for IES, aiming to minimize the total cost over the dispatch cycle. Furthermore, an optimal scheduling algorithm based on approximate dynamic programming (ADP) was designed to solve this model. Numerical experiments reveal that, while ensuring user comfort, the proposed real-time scheduling scheme, by comprehensively considering the interactions among various system inputs, significantly enhances system flexibility and economic performance. It effectively tackles the uncertainty of RE, thereby improving energy utilization efficiency.

Keywords Carbon emissions, Approximate dynamic programming, Demand response, Real-time scheduling

AMS 2010 subject classifications 90B35, 90C90

DOI: 10.19139/soic-2310-5070-2217

1. Introduction

Smart grids (SG) are at the core of the future power system, leveraging advanced information, communication, and control technologies to supply electricity from power plants to active consumers in a controlled and intelligent manner [1]. As confirmed by some recent studies [2, 3, 4], SG is combined with an integrated energy systems (IES, which is a single entity for the integration of distributed energy sources within the local energy system). It enables efficient, real-time, and flexible dispatch of diverse energy sources, including electricity, cooling, and heating, to tackle the challenges of growing global energy demand and structural diversification [5, 6]. In reality, it is also widely adopted in industrial parks, urban areas, and public buildings, driven by numerous smart energy dispatch models.

Along with the accessibility of SG, coupled with advancements in smart home technologies, and the implementation of time-varying energy pricing models, the establishment of IES in SG is imminent, both economically and environmentally speaking. This integration fosters effective energy utilization, and has the potential to reduce carbon emissions, strengthen energy security and operational flexibility. Extensive works have researched on modeling and optimizing the dispatch of IES [7, 8].

*Correspondence to: Xiaoyun Tian (Email: xiaoyun_txy@163.com). Institute of Operations Research and Information Engineering, Beijing University of Technology, Beijing, China (100124).
[a] These authors contributed equally to this work.

ISSN 2310-5070 (online) ISSN 2311-004X (print)

Zhou et al. [7] proposed a day-ahead scheduling strategy for an IES in the context of joint energy and ancillary service markets, which takes into account the uncertainty of energy market prices and renewable energy (RE) (e.g., wind power and solar power generation, which can be represented by the abbreviations of wind turbine and photovoltaic, WT and PV). To address these challenges, Wang et al. [8] quantitatively defined the fluctuations and uncertainty of IES, exemplified by the application of energy storage systems, which is also aimed at mitigating climate change and enhancing the penetration of RE. Guo et al. [9] developed an economic-environmental dispatch scheme for IES of industrial energy park using a hybrid approach, with the objective of minimizing the total operating costs of energy parks and reducing carbon dioxide emissions. With the development of artificial intelligence (AI), many scholars use AI-assisted methods to study problems, such as [10, 11, 12, 13, 14].

As mentioned, incorporating numerous RE units into the IES within SG, while offering flexibility and sustainability, can lead to significant power fluctuations due to the intermittency, uncertainty, etc. of RE. Day-ahead scheduling and real-time scheduling are important parts of the operation and management of the power system to ensure its safe, stable and efficient operation. For example, to handle the uncertainties of RE resources and variety load demands, Cheng et al. [15] proposed a multi-time scale dynamic robust optimal scheduling strategy to minimize the intraday operating cost. To better compensate for the unpredicted disturbances and incorporate the real-time information, they also introduced a rolling optimization strategy to adjust the real-time power deviation. The main difference between the two is that the former scheduling cycle is 24h, which provides guidance for the operation of the power system on the following day. The latter is more delicate in terms of time scale and needs to be based on the ultra-short-term forecast data of new energy and load, and responds quickly to sudden failures by adjusting the power generation output, cutting load and other measures [16].

Essentially, real-time scheduling poses as a multi-stage sequential optimisation problem, requiring optimal decisions at each stage based on current states and future predictions. Dynamic programming (DP), a prevalent approach to tackle this, enabling the construction of scheduling strategies that swiftly adapt to uncertainties and offer optimal solutions [17]. However, its applicability diminishes with large-scale problems due to the fact that we have to loop overall the possible states, decisions and outcomes in the state space. Accordingly, approximate dynamic programming (ADP), by incorporating approximation techniques, can effectively reduce computational complexity and sacrificing optimality for faster solution speed within an acceptable range [18].

With consideration of the uncertainty of long-term system load growth and short-term power fluctuations, Sun et al. [19] presented a flexible distribution system expansion planning model. Based on the ADP idea, they decomposed the original multi-stage optimization problem into successive subproblems to simplify the complex solution process. Similarly, Korkas et al. [20] developed an intelligent distributed control approach, which utilize a feedback-based optimization scheme, to get the optimal energy dispatch and operation cost of grid connected buildings. Pan et al. [21] employed an improved ADP approach to investigate risk-averse real-time dispatch within integrated power and heat systems.

For the dynamic process of combined-cycle gas turbine, Lin et al. [16] proposed a new real-time optimization algorithm based on ADP, which was experimentally shown to be superior to other algorithms in terms of economy and computational efficiency. Liang et al. [22] devised an improved ADP algorithm that account for coupled source-output and load-demand power balance among multiple adjacent time intervals. Zhao et al. [18] tailored state-space approximate dynamic programming (SS-ADP) to quickly generate day-ahead functions and solve smart home energy management problems via the Bellman equation [23]. Pan et al. [24] investigated the real-time dispatch of IES with thermal and electrical storages, using a hybrid approach combining stochastic dynamic programming and imitation learning. The approach tackles high dimensions of stochasticity and complexity by utilizing value function monotonicity, and imitative learning to facilitate off-line pre-learning.

To address the intermittency and uncertainty of RE in SG, we have devised a comprehensive scheduling model for IES, incorporating strategies such as demand response (DR) [25]. This model not only leverages clean energy sources like PV and WT but also accounts for factors like carbon dioxide emissions and DR, striving for more environmentally friendly and cost-effective energy management. Among them, DR serves as a pivotal tool of demand-side management, guiding users to adjust their energy consumption patterns. This, in turn, fosters synergy among multi-energy synergy within the IES, enabling a more agile response to fluctuations in energy supply and demand. The proposed optimal dispatch algorithm in our work dynamically adjusts the operational states of

various energy equipment, enabling intelligent real-time scheduling that minimizes total costs within the scheduling horizon. The main contributions of this paper are as follows:

- A novel multi-energy system scheduling model integrating RE utilization, environmental impacts, and DR mechanisms is proposed, which provides a comprehensive view of IES scheduling.
- Based on the ADP method, an efficient optimal scheduling algorithm capable of intelligent real-time scheduling is designed. By dynamically adjusting the operating strategies of gas turbine (GT), battery storage (BS), thermal storage (TS), PV, and WT, the algorithm adapts to the ever-changing energy supply and demand scenarios.
- Experimental results demonstrate that our proposed method can effectively schedule various energy supply devices to meet both electrical and thermal load demands, while guaranteeing the comfort of the users, as well as significantly reducing the the operating cost of IES and improve the energy efficiency.

The rest of this paper is organized as follows. The mathematical model and real-time dispatch framework of IES are presented in Section 2. In Section 3, we design a new algorithm as well as analysis for the proposed model. Section 4 conducts case studies. In Section 5, we draw conclusions.

2. Model

This section begins with an overview of the architecture of an IES in SG, which is capable of delivering both thermal and electrical energy. Subsequently, from a technical point of view, it describes all the constraints associated with each component included in our model.

2.1. The structure of IES

In SG, given the intermittency and uncertainty, we have devised an IES incorporating diverse energy sources. This is realized by deploying GT, PV, WT and other energy devices to provide heat and electricity. Figure 1 illustrates the IES configuration. To enhance the complementarity of various energy sources and improve the flexibility and reliability of the IES, a multi-level scheduling model is developed. This model integrates DR into an effective load management strategy, alongside a carbon reduction strategy aimed at optimizing the energy mix, effectively reducing energy consumption and carbon emissions.

The model aims to optimize the scheduling of electricity and thermal energy, minimize system operational costs while ensure energy load demands are met, through coordinated dispatching of various energy devices. It provides real-time scheduling solutions. The objective function is to minimize the total costs incurred within the scheduling period, encompassing costs associated with grid, BS, TS, PV, WT, GT, EH, DR and carbon emissions.

2.2. Constraints

(1) Energy storage It consists of two types of devices: BS and TS. This model can solves the conflict between energy supply and demand, and improves the security and stability of the IES by capturing excess energy generated during peak periods and releasing it during high demand or low peak periods.

Electrical storage For BS-based electrical energy storage, the following constraints are satisfied.

$$0 \leqslant P_{\mathrm{ch},t}^{\mathrm{BS}} \leqslant a_{\mathrm{ch},t}^{\mathrm{BS}} P_{\mathrm{max,ch}}^{\mathrm{BS}}, \forall t \in \mathcal{T}, \tag{1}$$

$$0 \leqslant P_{\mathrm{dc}}^{\mathrm{BS}} \leqslant a_{\mathrm{dc},t}^{\mathrm{BS}} P_{\mathrm{max,dc}}^{\mathrm{BS}}, \forall t \in \mathcal{T}, \tag{2}$$

$$a_{\mathrm{dc},t}^{\mathrm{BS}} + a_{\mathrm{ch},t}^{\mathrm{BS}} \leqslant 1, \forall t \in \mathcal{T}, \tag{3}$$

where the battery charging and discharging power is constrained by the upper and lower limits in Eq. (1)-(2), and cannot be charged and discharged simultaneously, yields Eq. (3).

Correspondingly, Eqs. (4)-(5) show the current energy level $E^{\mathrm{BS},t}$ of BS and its capacity limits at time t. Specifically, Eq. (4) shows the variation of energy stored in BS, where the amount of electricity stored in the

Nomenclature

Indices

Δt	Time interval

Abbreviations

ADP	Approximate dynamic programming
BS	Battery storage
TS	Thermal storage
PV	Photovoltaic power generation
WT	Wind turbine power generation
GT	Gas turbine
EH	Electricity to heat equipment

Binary variables

$a^{\mathrm{BS}}_{\mathrm{ch/dc},t}$	State of charging/discharging at t-th time slot, 0(off)/1(on)
$a^{\mathrm{TS}}_{\mathrm{ch/dc,t}}$	State of absorbing/releasing heat energy, 0(off)/1(on)
a^{GT}_t	Integer variables representing the operational state of GT, 0(off)/1(on)
$u(t)$	Binary variable of generator, 1 if on otherwise 0

Variables

$P^{\mathrm{BS}}_{\mathrm{ch/dc},t}$	Charging/discharging power of BS at time-slot t
E^{BS}_t	Energy stored in BS at time-slot t
$H^{\mathrm{TS}}_{\mathrm{ch/dc},t}$	Absorbing/releasing power of TS
E^{TS}_t	Energy stored in TS at time-slot t
$P^{\mathrm{PV/WT}}_t$	Output power of the PV panels/wind turbine
P^{grid}_t	Purchased amount of power from grid
P^{GT}_t	Output power of gas turbine
H^{GT}_t	Generated heat of gas turbine
H^{EH}_t	Heat power generated by EH
P^{EH}_t	Electricity power used to generated heat by EH
P^{IL}_t	Interrupted electrical load for time period t
$P^{\mathrm{load}}_{\mathrm{ini},t}$	Initial electrical load in time-slot t

Sets and parameters

ε^{grid}_t	Purchase price of electricity from the grid
$L^{\mathrm{Power}}(t)$	Electrical load
$L^{\mathrm{Heat}}(t)$	Thermal load
$P^{\mathrm{BS}}_{\mathrm{max,ch/dc}}$	Maximum charging/discharging power of BS
$E^{\mathrm{BS}}_{\mathrm{max\,/\,min}}$	Upper/lower limit of power stored in BS
η^{BS}	Energy loss factor of BS
$\eta^{\mathrm{BS}}_{\mathrm{ch/dc}}$	Chagrining/discharging efficiency of BS
$\varepsilon^{\mathrm{BS/TS}}$	Operation cost coefficient of BS/TS
$H^{\mathrm{TS}}_{\mathrm{max,ch/dc}}$	Maximum absorbing/releasing power of TS
$E^{\mathrm{TS}}_{\mathrm{max\,/\,min}}$	Upper/lower limit of energy stored in TS
η^{TS}	Energy loss factor of TS
$\eta^{\mathrm{TS}}_{\mathrm{ch/dc}}$	Absorbing/releasing efficiency of TS
η^{pv}	Power generation efficiency of PV
S^{pv}	The area of PV
$I^{\mathrm{pv}}(t)$	Uncertain solar radiation parameter
T^{out}_t	Outdoor temperature of building at time slot t (°C)
η^{GT}_e	Electrical efficiency of gas turbine
λ	Heat value of natural gas
η^{GT}_h	Heat efficiency of gas turbine
$P^{\mathrm{GT}}_{\mathrm{max\,/\,min}}$	Maximum/Minimum output generated power of GT
$P^{\mathrm{RD/RU}}_{\mathrm{min}}$	Maximum ramp-down/ramp-up power of generator
$\varepsilon^{\mathrm{GT}}$	Operation cost coefficient of GT
$\varepsilon^{\mathrm{PV/WT}}$	Operation cost coefficient of PV/Wind turbine
$P^{\mathrm{PV/WT}}_{\mathrm{max},t}$	Maximum generate power of PV/Wind turbine
$P^{\mathrm{grid}}_{\mathrm{max}}$	Maximum purchased amount of power from grid
η^{EH}	Electricity to heat efficiency
$\varepsilon^{\mathrm{EH}}$	Opeartion cost of EH
$k_{\mathrm{GT/grid}}$	Carbon emission of GT/grid
$\varepsilon^{\mathrm{CO_2}}$	Unit cost of carbon emission
$\varepsilon^{\mathrm{DR}}$	Unit penalties for DR
$P^{\mathrm{IL}}_{\mathrm{max}}$	Maximum interruptable electricity load
$P^{\mathrm{load}}_{\mathrm{max}}$	Maximum initial electricity load

current moment is related to the previous moment, which includes: the first term, the actual power after charging and discharging at t-th time slot; and the second term, the remaining stored power at $t-1$. The capacity of BS

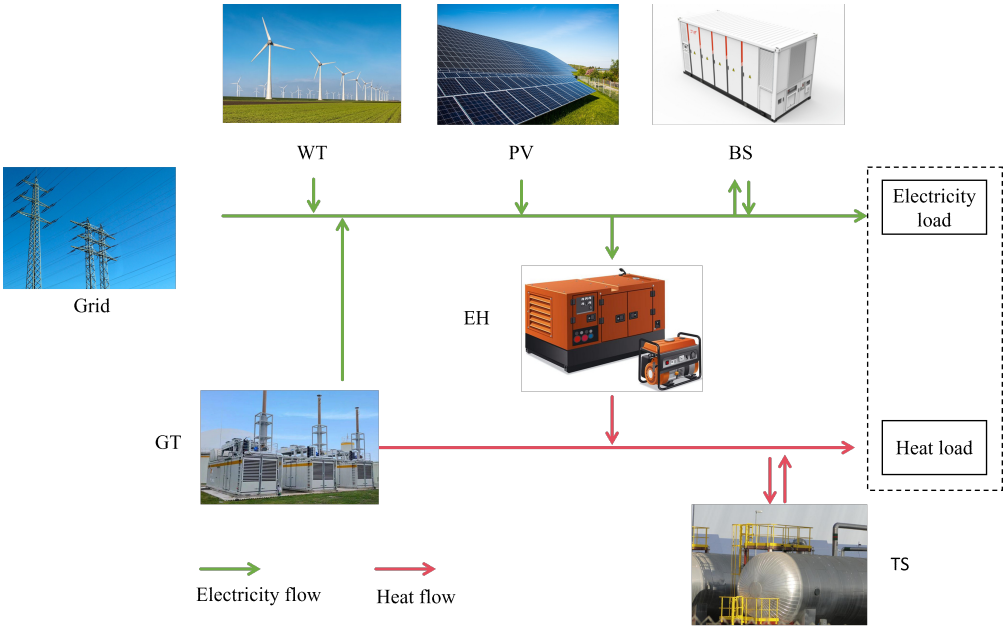

Figure 1. IES structure diagram.

cannot exceed its minimum/maximum in Eq. (5).

$$E_t^{\mathrm{BS}} = \left(\eta_{\mathrm{ch},t}^{\mathrm{BS}} P_{\mathrm{ch},t}^{\mathrm{BS}} - \frac{P_{\mathrm{dc},t}^{\mathrm{BS}}}{\eta_{\mathrm{dc}}^{\mathrm{BS}}}\right)\Delta t + (1-\eta^{\mathrm{BS}})E_{t-1}^{\mathrm{BS}}, \forall t \in \mathcal{T}, \tag{4}$$

$$E_{\min}^{\mathrm{BS}} \leqslant E_t^{\mathrm{BS}} \leqslant E_{\max}^{\mathrm{BS}}, \forall t \in \mathcal{T}. \tag{5}$$

Therefore, the operating cost of BS is derived as follows:

$$C_t^{\mathrm{BS}} = \varepsilon^{\mathrm{BS}}\left(P_{\mathrm{ch},t}^{\mathrm{BS}} + P_{\mathrm{dc},t}^{\mathrm{BS}}\right)\Delta t, \forall t \in \mathcal{T}. \tag{6}$$

Thermal storage Similar to BS, TS is used to capture surplus heat energy over a period of time and releases it into the system when required.

$$0 \leqslant H_{\mathrm{ch},t}^{\mathrm{TS}} \leqslant a_{\mathrm{ch},t}^{\mathrm{TS}} H_{\mathrm{max,ch}}^{\mathrm{TS}}, \forall t \in \mathcal{T}, \tag{7}$$

$$0 \leqslant H_{\mathrm{dc},t}^{\mathrm{TS}} \leqslant a_{\mathrm{dc},t}^{\mathrm{TS}} H_{\mathrm{max,dc}}^{\mathrm{TS}}, \forall t \in \mathcal{T}, \tag{8}$$

$$a_{\mathrm{ch},t}^{\mathrm{TS}} + a_{\mathrm{dc},t}^{\mathrm{TS}} \leqslant 1, \forall t \in \mathcal{T}. \tag{9}$$

The absorbing/releasing heat of TS is constrained by its lower and upper bounds in Eqs. (7)-(8), and it also cannot absorb and release heat simultaneously, yields Eq. (9).

$$E_t^{\mathrm{TS}} = \left(\eta_c^{\mathrm{TS}} H_{\mathrm{c},t}^{\mathrm{TS}} - \frac{H_{\mathrm{d},t}^{\mathrm{TS}}}{\eta_d^{\mathrm{TS}}}\right)\Delta t + \left(1-\eta^{\mathrm{TS}}\right)E_{t-1}^{\mathrm{TS}}, \forall t \in \mathcal{T}, \tag{10}$$

$$E_{\min}^{\mathrm{TS}} \leqslant E^{\mathrm{TS},t} \leqslant E_{\max}^{\mathrm{TS}}, \forall t \in \mathcal{T}. \tag{11}$$

The existing energy capacity of storage in Eq. (10), is dependent on prior energy level of the storage E_{t-1}^{TS}, the absorbing heat with efficiency η_{ch}^{TS} and the releasing heat η_{dc}^{TS}. To protect the equipment, the storage capacity of TS must strictly follow Eq. (11).

Thus, the operating cost of TS is:

$$C_t^{\mathrm{TS}} = \varepsilon^{\mathrm{TS}} \left(P_{\mathrm{ch},t}^{\mathrm{TS}} + P_{\mathrm{dc},t}^{\mathrm{TS}} \right) \Delta t, \forall t \in \mathcal{T}. \tag{12}$$

(2) Renewable energy It provides clean energy for IES operation. We consider two types of RE generation equipments: WT and PV. Due to the limitations of the devices, the following constraints are imposed on the output power.

$$0 \leq P_t^{\mathrm{PV}} \leq P_{\max}^{\mathrm{PV}}, \forall t \in \mathcal{T}, \tag{13}$$
$$0 \leq P_t^{\mathrm{WT}} \leq P_{\max}^{\mathrm{WT}}, \forall t \in \mathcal{T}, \tag{14}$$

where P_t^{PV} and P_t^{WT} are the generated power of PV and WT, respectively. Therefore, the cost of generating RES include the above two components, i.e.

$$C_t^{\mathrm{RES}} = \varepsilon^{\mathrm{PV}} P_t^{\mathrm{PV}} + \varepsilon^{\mathrm{WT}} P_t^{\mathrm{WT}}, \forall t \in \mathcal{T}. \tag{15}$$

(3) Grid Our model is capable of exchanging power with the grid to meet demand. Specifically, the power purchased from the grid satisfies the constraint in Eq. (16). It is noteworthy that electricity prices, denoted by $\varepsilon_t^{\mathrm{grid}}$, vary over time as shown in Table 1. Eq. (17) is the cost of purchasing electricity.

$$0 \leq P_t^{\mathrm{grid}} \leq P_{\max}^{\mathrm{grid}}, \forall t \in \mathcal{T}, \tag{16}$$
$$C_t^{\mathrm{grid}} = \varepsilon_t^{\mathrm{grid}} P_t^{\mathrm{grid}}, \forall t \in \mathcal{T}. \tag{17}$$

Table 1. Grid TOU price.

Periods	Specific time	Purchase(CNY)
Valley	1-7, 24	0.4
Flat	8, 12-18	0.5
Peak	9-11, 19-23	0.7

(4) Gas turbine During the GT process, substantial amounts of high-temperature waste heat is generated, which is converted into hot water or steam for heating through the circulating medium within the flue gas heat exchanger. It is often used as a peaking device to further relieve the IES of heat, power stress and peaking needs.

$$a_t^{\mathrm{GT}} P_{\min}^{\mathrm{GT}} \leq P_t^{\mathrm{GT}} \leq a_t^{\mathrm{GT}} P_{\max}^{\mathrm{GT}}, \forall t \in \mathcal{T}, \tag{18}$$
$$a_t^{\mathrm{GT}} P_{\min}^{\mathrm{RD}} \leq P_t^{\mathrm{GT}} - P_{t-1}^{\mathrm{GT}} \leq a_t^{\mathrm{GT}} P_{\max}^{\mathrm{RU}}, \forall t \in \mathcal{T}, \tag{19}$$
$$H_t^{\mathrm{GT}} = \frac{P_t^{\mathrm{GT}}}{\eta_e^{\mathrm{GT}}} \eta_h^{\mathrm{GT}}, \forall t \in \mathcal{T}, \tag{20}$$
$$C_t^{GT} = \frac{\varepsilon^{GT}}{\eta_e^{GT} \lambda} P_t^{GT}, \forall t \in \mathcal{T}, \tag{21}$$

where a_t^{GT} is a binary variable showing the status of GT (on–off). Eq. (18) implies the range of fluctuations in GT generation P_t^{GT} at time period t. The symbols $P_{\max}^{\mathrm{RU}}$ and $P_{\min}^{\mathrm{RD}}$ in Eq. (19) are upper and lower allowable rates of the GT climbing. Correspondingly, the heat generated by GT in the power generation process is given by Eq. (20), where η_e^{GT} is the power generation efficiency of GT and η_h^{GT} is the heat generation efficiency. Therefore, the cost of GT is in Eq. (21).

(5) Electricity-to-heat To cater to the demand for heat energy supply from end-users on the demand side, flexible electric-to-heat devices, such as electric heaters and electric boilers, are indispensable.

$$0 \leq P_t^{\mathrm{EH}} \leq P_{\max}^{\mathrm{EH}}, \forall t \in \mathcal{T}, \tag{22}$$
$$H_t^{\mathrm{EH}} = \eta^{\mathrm{EH}} P_t^{\mathrm{EH}}, \forall t \in \mathcal{T}, \tag{23}$$
$$C_t^{\mathrm{EH}} = \varepsilon^{\mathrm{EH}} P_t^{\mathrm{EH}}, \forall t \in \mathcal{T}, \tag{24}$$

where the symbol η^{EH} is the electric-heat ratio of EH. The electric-heat conversion relationship is in Eq. (23) , and its cost is in Eq. (24).

(6) Carbon emission mechanism It encompasses both the grid and GT carbon emissions, with the aim of incentivizing energy producers and consumers to reduce the use of fossil fuels and increase the adoption of RE.

$$C_t^{CO_2} = \varepsilon^{CO_2} \left(k_{\mathrm{GT}} P_t^{\mathrm{GT}} + k_{\mathrm{grid}} P_{\mathrm{b},t}^{\mathrm{grid}} \right), \forall t \in \mathcal{T}, \tag{25}$$

where $k_{\mathrm{GT/grid}}$ is CO_2 emissions per unit of electricity generated in the GT/grid, and $P_{\mathrm{b},t}^{\mathrm{grid}}$ denote the amount of electrical power purchased by IES from the main grid at t-th time slot.

(7) Demand response During peak periods of electricity consumption, users would stop power consumption according to the relevant incentive policies of SG to alleviate the pressure of power supply during peak periods and reduce their own energy consumption costs. The relevant constraints for interruptible loads (IL) can be described as follows:

$$0 \leqslant P_t^{\mathrm{IL}} \leqslant P_{\max}^{\mathrm{IL}}, \forall t \in \mathcal{T}, \tag{26}$$
$$0 \leq P_t^{\mathrm{load}} = P_{\mathrm{ini},t}^{\mathrm{load}} - P_t^{\mathrm{IL}} \leq P_{\max}^{\mathrm{load}}, \forall t \in \mathcal{T}, \tag{27}$$
$$C_t^{\mathrm{DR}} = \varepsilon^{\mathrm{DR}} P_t^{\mathrm{IL}}, \forall t \in \mathcal{T}, \tag{28}$$

where P_T^{load} and $P_{\mathrm{ini},t}^{\mathrm{load}}$ imply the total actual (after DR) and initial (before DR) power loads in the period t, respectively. Eqs. (26) and (27) ensure that end-users have limited IL in per unit time and needs to meet certain load demand.

(8) Energy balance The balance between supply and demand of multiple energies needs to be satisfied while reducing the operating cost of IES. The following are the constraints on the balance of supply and demand for electricity and heat that should be met by IES.

Power balance The left term is the total power supply, and the right is the total demand.

$$P_t^{\mathrm{GT}} + P_t^{\mathrm{PV}} + P_t^{\mathrm{WT}} + P_t^{\mathrm{grid}} + P_{\mathrm{dc},t}^{\mathrm{BS}} = P_t^{\mathrm{load}} + P_{\mathrm{ch},t}^{\mathrm{BS}} + P_t^{\mathrm{EH}}, \forall t \in \mathcal{T}. \tag{29}$$

Heat balance Similar to Eq. (29), the left equation is the total heat supply and the right is the heat demand.

$$H_t^{\mathrm{EH}} + H_t^{\mathrm{GT}} + H_{\mathrm{dc},t}^{\mathrm{TS}} = H_{\mathrm{ch},t}^{\mathrm{TS}} + H_t^{\mathrm{load}}, \forall t \in \mathcal{T}. \tag{30}$$

2.3. Objective funtion

For the IES, there hope to meet various energy requirements with as little cost as possible. Therefore, the objective function is to minimize the total cost within one cycle (set $|\mathcal{T}| = 24$ hours):

$$F = \min_X \sum_{t \in \mathcal{T}} C_t, \tag{31}$$

where C_t is the objective function in time $t \in \mathcal{T}$ and denote as

$$C_t = C_t^{\mathrm{BS}} + C_t^{\mathrm{TS}} + C_t^{\mathrm{RES}} + C_t^{\mathrm{grid}} + C_t^{\mathrm{GT}} + C_t^{\mathrm{EH}} + C_t^{\mathrm{CO_2}} + C_t^{\mathrm{DR}}.$$

3. Algorithm and analysis

(1) **IES state** It comprises external uncertain information W_t and the resource state R_t at each time $t \in \mathcal{T}$, i.e. $S_t = \{W_t, R_t\}$.

The symbol W_t is used to portray exogenous uncertainty information at the moment t, as shown in Eq. (32). In this context, electrical, and heat loads, maximum PV/WT output, and real-time prices are assumed to be stochastic, with their actual values unknown to IES in advance. The resource state R_t is the energy stored in TS and BS at time period t as shown in Eq. (33).

$$W_t = \left\{ \varepsilon_t^{\text{grid}}, P_{\text{ini},t}^{\text{load}}, H_t^{\text{load}}, P_{\max,t}^{PV}, P_{\max,t}^{WT} \right\}, \tag{32}$$

$$R_t = \left\{ E_t^{TS}, E_t^{BS} \right\}. \tag{33}$$

(2) **Decision variable** At time-slot t, the IES operator makes decisions based on the realized stochastic factors at the current stage and their future uncertainties. The real-time dispatch decision X_t is defined as,

$$X_t = \left\{ P_t^{\text{grid}}, P_t^{\text{PV}}, P_t^{\text{WT}}, P_t^{\text{GT}}, P_{\text{ch},t}^{\text{BS}}, P_{\text{dc},t}^{\text{BS}}, P_t^{\text{EH}}, H_t^{\text{GT}}, H_{\text{ch},t}^{\text{TS}}, H_{\text{dc},t}^{\text{TS}}, a_{\text{ch},t}^{\text{BS}}, a_{\text{dc},t}^{\text{BS}}, a_{\text{ch},t}^{\text{TS}}, a_{\text{dc},t}^{\text{TS}}, a_t^{\text{GT}}, P_t^{\text{IL}} \right\}.$$

(3) **State transition** Once the status of IES and scheduling decisions are known, the state transition can be defined as follows:

$$E^{\text{BS}}(t) = (1 - \eta_{\text{BS}}) E^{\text{BS}}(t-1) + \left(\eta_{\text{BS,c}} P_{\text{c}}^{\text{BS}}(t) - \frac{P_{\text{d}}^{\text{BS}}(t)}{\eta_{\text{BS,d}}} \right) \Delta t, \forall t \in \mathcal{T},$$

$$E^{\text{TS}}(t) = (1 - \eta_{\text{TS}})\, E^{\text{TS}}(t-1) + \left(\eta_{\text{TS},c} H_{\text{c}}^{\text{TS}}(t) - \frac{H_{\text{d}}^{\text{TS}}(t)}{\eta_{\text{TS},d}} \right) \Delta t, \forall t \in \mathcal{T}.$$

Therefore, the optimal policy at time-slot t can be determined by solving the following equation,

$$X_t = \arg\min_{X_t} C_t. \tag{34}$$

Based on the ADP algorithm, we proposed a new algorithm which focus on the optimal strategy for the current moment to solve the IES model. The procedures of real-time IES dispatch are shown in Figure 2. After recognizing the state information of the IES, the algorithm reacts to any realization of exogenous information and obtains near-optimal real-time scheduling by solving Eq. (34) step by step.

The detailed algorithm is described in Algorithm 1. It iterates with an hourly time step, initializing at $t := 1$ and then proceeding through the iterative process. In each iteration, it takes in the current state at that moment and solves a cost minimization problem to obtain scheduling decisions based on the current external and state information. Following this, the system state is updated according to the obtained decisions, and the process iterates until the completion of the 24-hour. Finally, the optimal solution calculated over the entire cycle is output. Compared with other algorithms, our algorithm does not need additional prediction information to obtain the best scheduling policy at each moment, so it is more suitable for real-time scheduling scenarios both computationally and operationally.

4. Case study

The test system of the IES consists of a variety of generation and storage components such as BS, TS, PV, WT, EH and grid. The test system configuration is presented in Table 2, and the electrical and heat loads are designed to reflect typical daily variations in IES. Figure 3 illustrates the 24-hour variation trends of electric and heat loads. In daily life, the price of electricity purchased from the grid varies over time, and the real-time electricity price are set in Table 1.

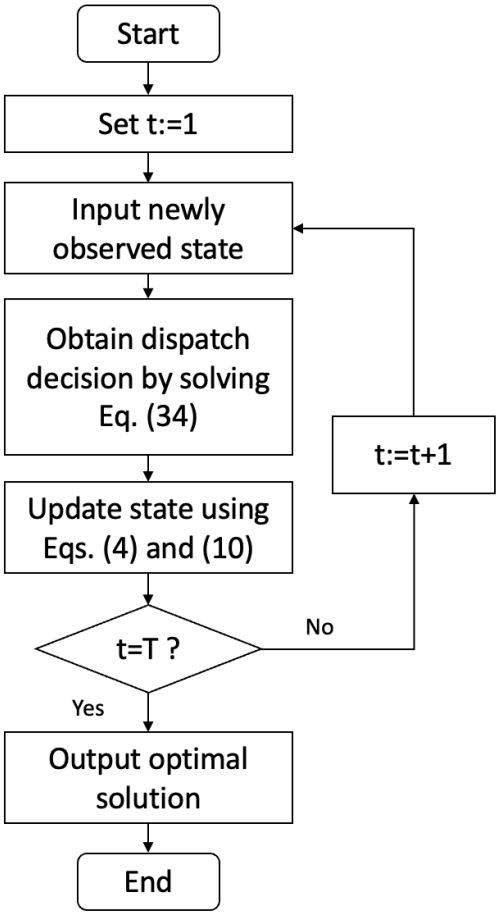

Figure 2. Optimal real-time dispatch flow diagram.

Under varying environmental conditions, the maximum power generation capacities of PV and WT systems differ significantly. The maximum power output for the PV system ($P^{PV}_{\max,t}$) is determined based on the irradiance levels during peak sunlight hours, typically occurring between 12:00 and 14:00. For this scenario, it is assumed that the PV system operates at a peak capacity of 700 kilowatts (kW) on sunny days. Similarly, the maximum output of WT ($P^{WT}_{\max,t}$) is based on optimal wind speeds, which are assumed to be 12 m/s, corresponding to a maximum generation of 600 kW.

The case study is actually implemented on VsCode 1.85.2 using Python 3.9 and CPLEX 22.1.1. The whole experiment is implemented on a PC with an Intel(R) Core(TM) i5-9300H CPU at 2.40GHz and 8 GB RAM.

4.1. Results analysis of energy dispatch

This section provides a comprehensive analysis of the energy dispatch results for a single day scenario, focusing on electrical and thermal energy conservation, state transitions of BS and TS, and detailed cost analysis of energy devices.

4.1.1. Electrical energy conservation Given the uncertainty of renewable energy (RE) and the scheduling capability of residential hubs, a key requirement for the IES is to keep a balance between supply and demand while ensuring user "comfort" (i.e., meeting normal demand). From Figure 4, the total electrical demand is satisfied by the combined output of the PV, WT, BS, GT and grid at each time t.

Algorithm 1 Optimal Real-time Dispatch

Input: Initial system state S_1, maximum time horizon T.

Output: Dispatch result $X = \{X_1, \ldots, X_T\}$.

$X \leftarrow \emptyset$.
for $t = 1$ **to** T **do**
    Step 1: State Formation
    Identify the external uncertain information W_t in Eq. (32).
    Measure the current resource state $R_t = \{E_t^{\mathrm{BS}}, E_t^{\mathrm{TS}}\}$ in Eq. (33).
    Obtain IES state $S_t \leftarrow \{W_t, R_t\}$.
    Step 2: Solve Optimal Decision
    $X_t \leftarrow \arg\min_{X_t \in \Pi_t} (C_t(S_t))$.
    Compute the cost function $C_t(S_t, X_t)$.
    Step 3: Update Resource State
    $E_{t+1}^{\mathrm{BS}} \leftarrow \left(\eta_{\mathrm{ch},t}^{\mathrm{BS}} P_{\mathrm{ch},t}^{\mathrm{BS}} - \frac{P_{\mathrm{dc},t}^{\mathrm{BS}}}{\eta_{\mathrm{dc}}^{\mathrm{BS}}}\right) \Delta t + (1 - \eta^{\mathrm{BS}}) E_t^{\mathrm{BS}}$.
    $E_{t+1}^{\mathrm{TS}} \leftarrow \left(\eta_c^{\mathrm{TS}} H_{c,t}^{\mathrm{TS}} - \frac{H_{\mathrm{d},t}^{\mathrm{TS}}}{\eta_d^{\mathrm{TS}}}\right) \Delta t + (1 - \eta^{\mathrm{TS}}) E_t^{\mathrm{TS}}$.
    Step 4: Update Decision
    $X \leftarrow X \cup \{X_t\}$.
end for
Output the complete set of dispatch decisions $X = \{X_1, \ldots, X_T\}$.

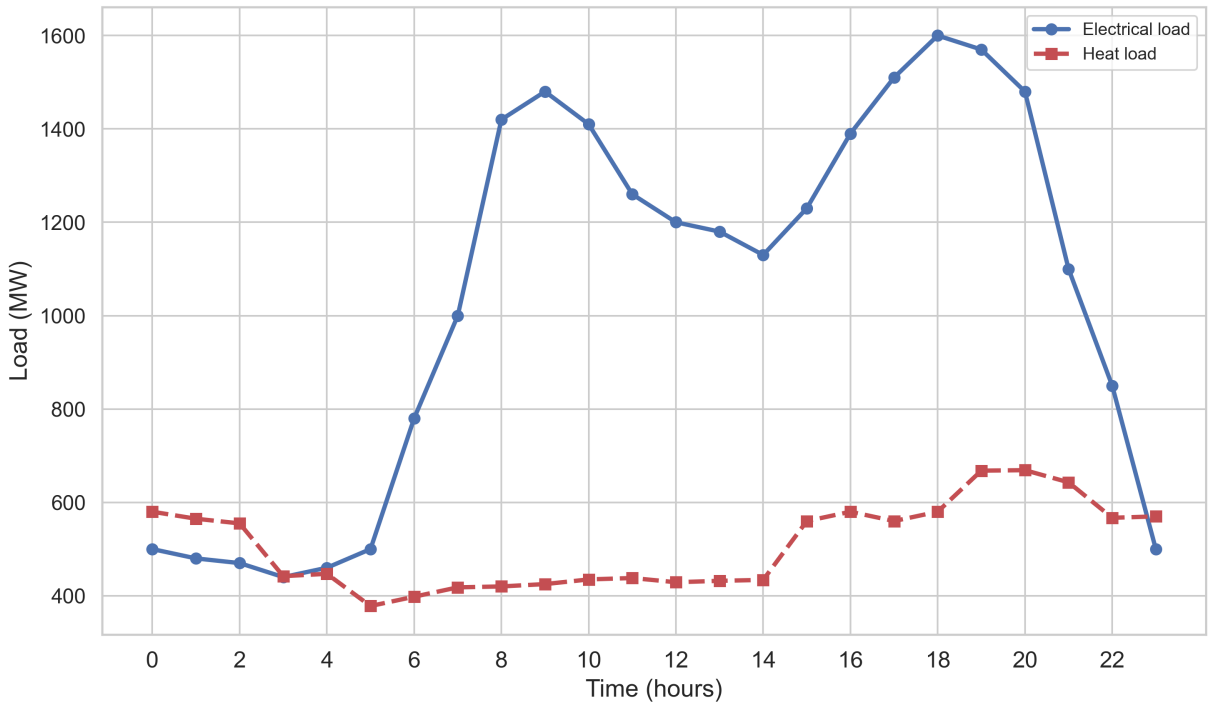

Figure 3. 24-hour variation of electric and heat load of PV and WT.

From Figure 5, it's obviously that the RES is the main power supply unit, accounting for 40%, followed by the grid 37%, GT 22% and BS 1%. For the electricity demand, in addition to the 67% of normal electricity demand,

Table 2. The configuration of the test system.

Parameter	Value	Parameter	Value
$P^{\mathrm{BS}}_{\mathrm{max,ch}}$	400 (kW)	$P^{\mathrm{BS}}_{\mathrm{max,dc}}$	400 (kW)
$E^{\mathrm{BS}}_{\mathrm{max}}$	1000 (kWh)	$E^{\mathrm{BS}}_{\mathrm{min}}$	400 (kWh)
$\eta^{\mathrm{BS}}_{\mathrm{ch}}$	0.96	$\eta^{\mathrm{BS}}_{\mathrm{dc}}$	0.96
η^{BS}	0.05	$\varepsilon^{\mathrm{BS}}$	0.01 (CNY/kWh)
$H^{\mathrm{TS}}_{\mathrm{max,ch}}$	600 (kW)	$H^{\mathrm{TS}}_{\mathrm{max,dc}}$	600 (kW)
$E^{\mathrm{TS}}_{\mathrm{max}}$	1000 (kWh)	$E^{\mathrm{TS}}_{\mathrm{min}}$	400 (kWh)
$\eta^{\mathrm{TS}}_{\mathrm{ch}}$	0.98	$\eta^{\mathrm{TS}}_{\mathrm{dc}}$	0.98
η^{TS}	0.05	ε^{TS}	0.05 (CNY/kWh)
$\varepsilon^{\mathrm{PV}}_{\mathrm{max}}$	0.1 (CNY/kWh)	$\varepsilon^{\mathrm{WT}}_{\mathrm{max}}$	0.1 (CNY/kWh)
$P^{\mathrm{grid}}_{\mathrm{max}}$	1000 (kWh)	$P^{\mathrm{GT}}_{\mathrm{max}}$	1000 (kWh)
$P^{\mathrm{RU}}_{\mathrm{max}}$	300 (kW)	$P^{\mathrm{RD}}_{\mathrm{min}}$	-300 (kW)
η^{GT}_{h}	0.3	η^{GT}_{e}	0.5
λ	8 (kWh/m^3)	$\varepsilon^{\mathrm{GT}}$	2.7 (CNY/m^3)
$P^{\mathrm{EH}}_{\mathrm{max}}$	1000 (kWh)	η^{EH}	0.8
$\varepsilon^{\mathrm{EH}}$	0.08 (CNY/kWh)	$\varepsilon^{\mathrm{CO_2}}$	0.1 (CNY/m^3)
k_{GT}	0.4 (kWh/m^3)	k_{grid}	0.5 (kWh/m^3)
$P^{\mathrm{IL}}_{\mathrm{max}}$	8 00 (kWh)	$P^{\mathrm{load}}_{\mathrm{max}}$	1500 (kWh)
$\varepsilon^{\mathrm{DR}}$	0.2 (CNY/kWh)		

31% of the electricity is used for heating, and only 2% of the electricity is storaged to BS. Considering the cost of energy storage equipment and energy loss, it is not cost-effective to equip mini-grids with BS devices, which can save the construction, operation and maintenance costs of the small-scale power grids.

4.1.2. Thermal energy conservation Figure 6 illustrates the 24-hour variation in thermal generation and consumption, and it's obvious that the IES can keep the balance under the model by adjusting TS, EH and GT. From Figure 7, it can be seen that the EH is the main heat supply unit accounting for 64%, followed by GT 33% and TS 3%. In the IES, the TS has a minimal impact on maintaining the balance between supply and demand. Considering the system configuration cost and operation cost of TS, it suggests that there is no need TS for the small-scale IES.

4.2. Demand response

In practical scenarios, IES cannot meet the demand indefinitely, due to the inherent functional limitations of the device. When the demand are out of the system's reach, then a demand response mechanism is needed to balance supply and demand. From Figure 8, it's obvious that the model can control normal operation within the system capacity range (1500kWh), which can ensure the safe operation of the IES.

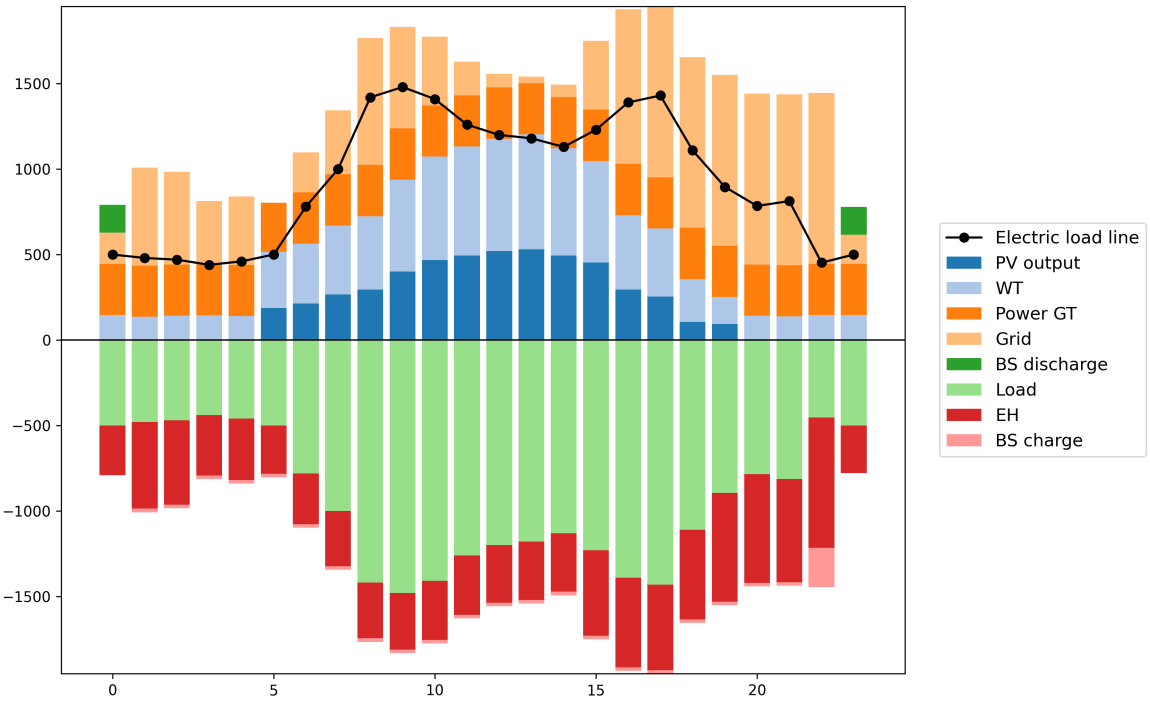

Figure 4. Electricity balance of optimal dispatch: 24-hour variation of electrical energy generation and consumption.

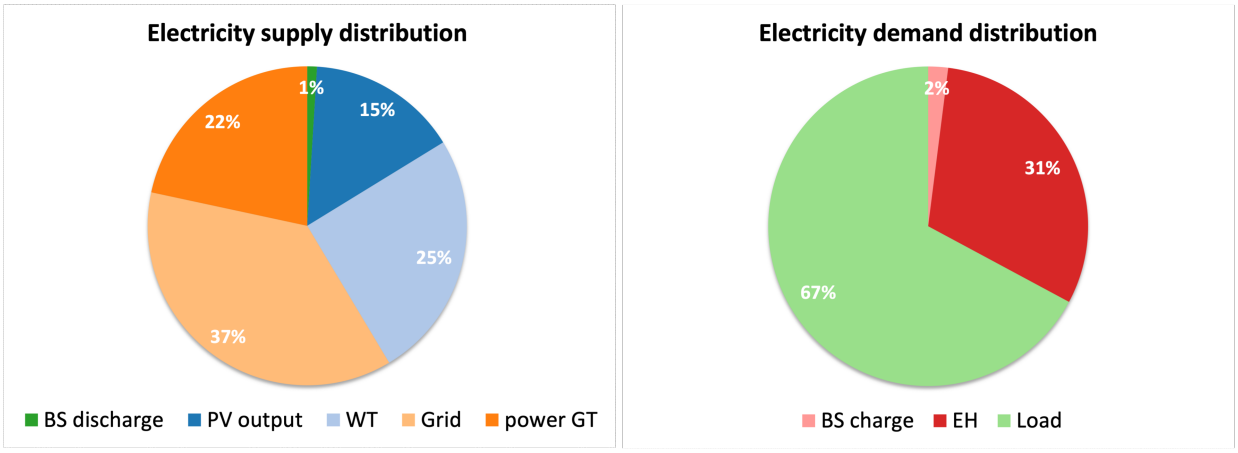

(a) (b)

Figure 5. Electricity energy composition proportion.

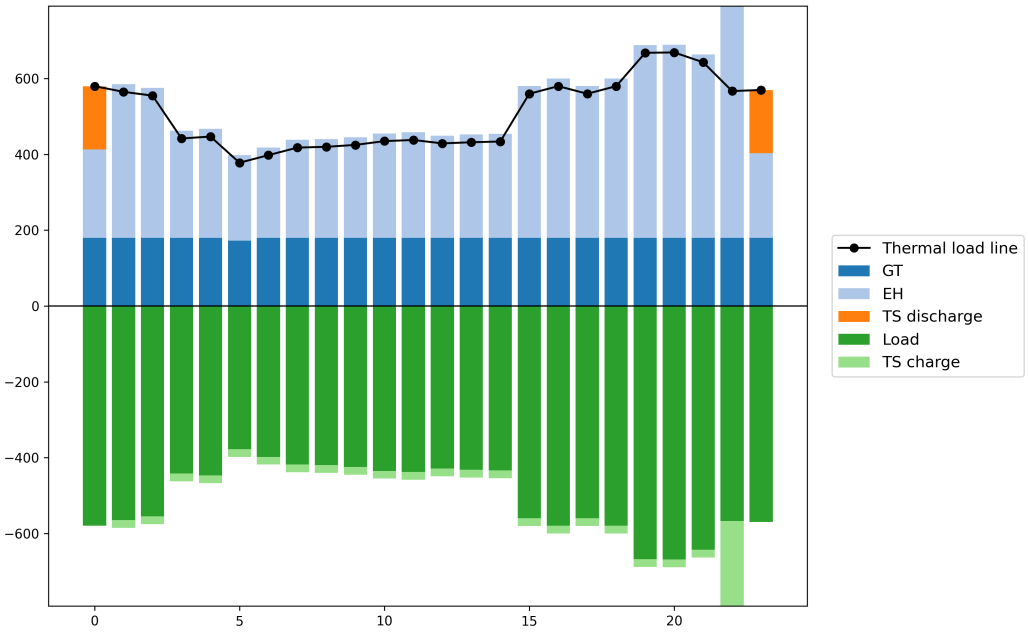

Figure 6. Thermal balance of optimal dispatch: 24-hour variation of thermal energy generation and consumption.

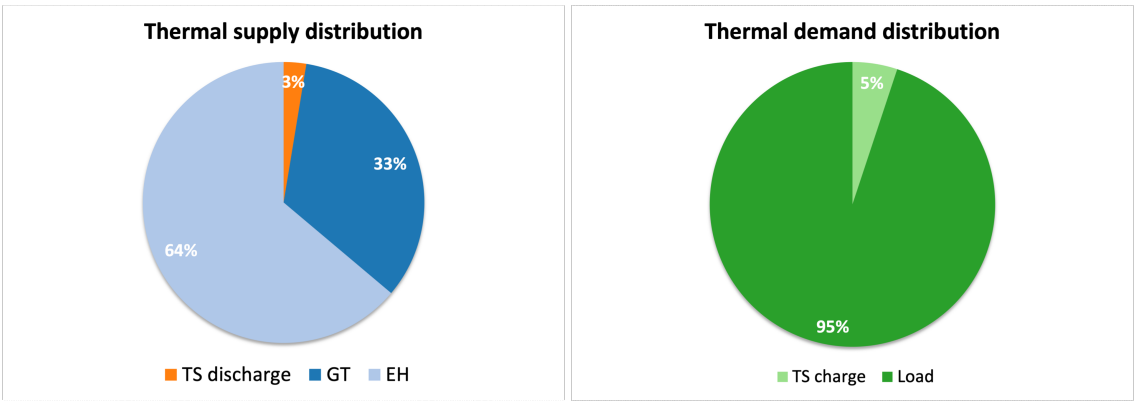

(a) (b)

Figure 7. Thermal energy composition proportion.

4.3. Cost analysis

The cost analysis for energy dispatch is presented in Table 3, which summarizes the operational costs for various energy devices, including electricity purchased from grid and released by BS, TS, PV, WT, GT and EH, and the penalty cost of DR. The results indicate that purchasing electricity from the grid incurs the highest cost, while discharging stored energy from BS and TS systems provides a cost-saving mechanism, particularly during peak demand periods.

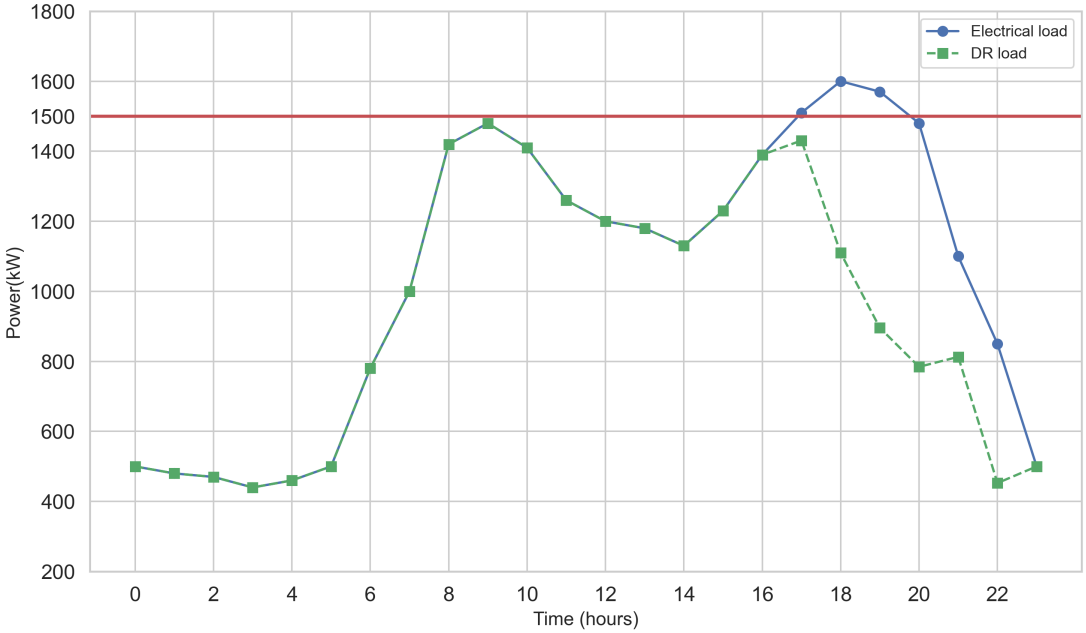

Figure 8. Energy dispatch of demand response.

Table 3. Cost analysis of energy devices for a single day scenario.

Energy device	Operational cost (CNY/kWh)
BS	9.9307
TS	49.3131
PV	507.0000
WT	836.8000
Grid	7241.7259
GT	4851.0682
EH	820.0801
CO2	901.5834
DR	2624.2466

5. Conclusion

The intermittency and uncertainty of the RES is a challenge to keep the stability of the IES. Real-time scheduling requires decisions to be made in a short period of time to respond to unexpected events. For these problem, this paper proposes a thermal-electric storage IES model, considering the DR mechanism and carbon emission mechanism, and employs an real-time programming to address the real-time dispatch problem of IES.

Dispatch results demonstrate the effectiveness of utilizing RE (e.g., PV and WT) in conjunction with energy generation system GT and EH, and energy storage system (BS and TS) to maintain energy balance and minimize the total operation costs. By combining the grid, GT and EH, IES can fully and safely utilize RE and maintain the energy balance. Under the DR mechanism, IES can safely and stably operation under its capacity. The results also show that the storage system are little useful in IES. Considering the economic befits, it may be better to not use storage system in small scale IES.

With the AI development, there are many researches study the combination of AI and ADP to solve the multi-stage stochastic decision problem. These can be used to further solve the real-time scheduling problem of IES.

Acknowledgements

The research is supported by National Key R&D Program of China (No. 2022YFE0196100).

REFERENCES

1. Siano P. Demand response and smart grids-A survey. Renewable and Sustainable Energy Reviews, 2014, 30: 461-478.
2. Xu Y, Zhang W, Liu W. Distributed dynamic programming-based approach for economic dispatch in smart grids. IEEE Transactions on Industrial Informatics, 2014, 11(1): 166-175.
3. Liang W, Lin S, Liu M, Wang Q, Xie Y, Sheng X. Stochastic economic dispatch of regional integrated energy system considering the pipeline dynamics using improved approximate dynamic programming. International Journal of Electrical Power & Energy Systems, 2022, 141: 108190.
4. Wu Y, Tian X, Gai L, Lim B H, Wu T, Xu D, Zhang Y. Energy management for PV prosumers inside microgrids based on Stackelberg–Nash game considering demand response. Sustainable Energy Technologies and Assessments, 2024, 68: 103856.
5. Zia M F, Benbouzid M, Elbouchikhi E, Muyeen S M, Techato K, Guerrero J M. Microgrid transactive energy: Review, architectures, distributed ledger technologies, and market analysis. IEEE Access, 2020, 8: 19410-19432.
6. Merkert L, Harjunkoski I, Isaksson A, Säynevirta S, Saarela A, Sand G. Scheduling and energy-industrial challenges and opportunities. Computers & Chemical Engineering, 2015, 72: 183-198.
7. Zhou Y, Wei Z, Sun G, Cheung K W, Zang H, Chen S. A robust optimization approach for integrated community energy system in energy and ancillary service markets. Energy, 2018, 148: 1-15.
8. Wang W, Yuan B, Sun Q, Wennersten R. Application of energy storage in integrated energy systems-A solution to fluctuation and uncertainty of renewable energy. Journal of Energy Storage, 2022, 52: 104812.
9. Guo Q, Nojavan S, Lei S, Liang X. Economic-environmental evaluation of industrial energy parks integrated with CCHP units under a hybrid IGDT-stochastic optimization approach. Journal of Cleaner Production, 2021, 317: 128364.
10. Chen J, Han J, Meng X, Li Y, Li H. Graph convolutional network combined with semantic feature guidance for deep clustering. Tsinghua Science and Technology, 2022, 27(5): 855-868.
11. Zhao K, Ning L. Hybrid navigation method for multiple robots facing dynamic obstacles. Tsinghua Science and Technology, 2022, 27(6): 894-901.
12. Yu D, Zou Y, Yu J, Zhang Y, Li F, Cheng, X., Dressler F, Lau F C. Implementing the abstract MAC layer in dynamic networks. IEEE Transactions on Mobile Computing, 2020, 20(5): 1832-1845.
13. Lin J, Feng S, Zhang Y, Yang Z, Zhang Y. A novel deep neural network based approach for sparse code multiple access. Neurocomputing, 2020, 382: 52-63.
14. Jiaming Hu, Boon-Han Lim, Xiaoyun Tian, Kang Wang, Dachuan Xu, Feng Zhang, Yong Zhang. A comprehensive review of artificial intelligence applications in the photovoltaic systems. CAAI Artificial Intelligence Research, 2024, 3(9150031): 1-16.
15. Cheng Z, Jia D, Li Z, Si J, Xu S. Multi-time scale dynamic robust optimal scheduling of CCHP microgrid based on rolling optimization. International Journal of Electrical Power & Energy Systems, 2022, 139: 107957.
16. Lin Z, Song C, Zhao J, Yin H. Improved approximate dynamic programming for real-time economic dispatch of integrated microgrids. Energy, 2022, 255: 124513.
17. Wu M, Xu J, Zeng L, Li C, Liu Y, Yi Y, Jiang Z. Two-stage robust optimization model for park integrated energy system based on dynamic programming. Applied Energy, 2022, 308: 118249.
18. Zhao Z, Keerthisinghe C. A fast and optimal smart home energy management system: State-space approximate dynamic programming. IEEE Access, 2020, 8: 184151-184159.
19. Sun Q, Wu Z, Gu W, Zhu T, Zhong L, Gao T. Flexible expansion planning of distribution system integrating multiple renewable energy sources: An approximate dynamic programming approach. Energy, 2021, 226: 120367.
20. Korkas C D, Terzopoulos M, Tsaknakis C, Kosmatopoulos E B. Nearly optimal demand side management for energy, thermal, EV and storage loads: An approxim dynamic programming approach for smarter buildings. Energy and Buildings, 2022, 255: 111676.
21. Pan Z, Yu T, Li J, Qu K, Yang B. Risk-averse real-time dispatch of integrated electricity and heat system using a modified approximate dynamic programming approach. Energy, 2020, 198: 117347.
22. Liang W, Lin S, Liu M, Wang Q, Xie Y, Sheng X. Stochastic economic dispatch of regional integrated energy system considering the pipeline dynamics using improved approximate dynamic programming. International Journal of Electrical Power & Energy Systems, 2022, 141: 108190.
23. Bellman R. Dynamic programming. Princeton University Press, Princeton, NJ, USA, 1958, 1: 3-25.
24. Pan Z, Yu T, Huang W, Wu Y, Chen J, Zhu K, Lu J. Real-time dispatch of integrated electricity and thermal system incorporating storages via a stochastic dynamic programming with imitation learning. International Journal of Electrical Power & Energy Systems, 2023, 153: 109286.
25. Dolatabadi A. Mohammadi-Ivatloo, B. Stochastic risk-constrained scheduling of smart energy hub in the presence of wind power and demand response. Applied Thermal Engineering, 2017, 123: 40-49.